Study of Dielectric Strength in EPDM by Nondestructive Dynamic Mechanical Analysis in High Electrical Field

F. G. Bonifacich[a], E. D. V. Giordano[a,b], O. A. Lambri[c], D. Gargicevich[a], R. R. Mocellini
CONICET-UNR, Laboratorio de Materiales (LEIM), Escuela de Ingeniería Eléctrica (EIE),
Centro de Tecnología e Investigación Eléctrica (CETIE), Facultad de Ciencias Exactas, Ingeniería y Agrimensura (FCEIA),
Av. Pellegrini 250, 2000, Rosario, Argentina
[a] CONICET's fellowship
[b] Instituto de Procesos Biotecnológicos y Químicos (IPROBYQ-CONICET), Facultad de Ciencias Bioquímicas y Farmacéuticas, Universidad Nacional de Rosario, Suipacha 531, S2002LRK Rosario, Argentina
[c] Member of the CONICET's Research Staff.

J. A. García[d], F. Plazaola[e]
Facultad de Ciencias y Tecnología, Universidad del País Vasco, UPV/EHU, Apdo. 644, 48080 Bilbao, País Vasco, Spain
[d] Departamento de Física Aplicada II and BC Materials (Basque Centre for Materials, Application and Nanostructures)
[e] Elektrika eta Elektronika Saila

F. A. Sánchez
División Física de Reactores Avanzados, Reactor Nuclear RA 6, Centro Atómico Bariloche, CNEA, Avda. Bustillo km 9.500, R8402AGP San Carlos de Bariloche, Argentina.

C. E. Boschetti[c] and P. E. Salvatori[a,f]
Instituto de Procesos Biotecnológicos y Químicos (IPROBYQ-CONICET), Facultad de Ciencias Bioquímicas y Farmacéuticas, Universidad Nacional de Rosario, Suipacha 531, S2002LRK Rosario, Argentina.
[f] Pampa Energía SA, Av. Juan D Peron 1000, 2202 Puerto General San Martín, Santa Fe, Argentina

ABSTRACT

In the present work the value of the degree of the area swept by the polymer chain due to an electrical force for a given mesostructure was related to the corresponding value of the dielectric strength. This value was deduced from the electric inclusion formalism applied to dynamic mechanical analysis (DMA) studies conducted under high electric field, which were performed in commercial ethylene-propylene-diene M-class rubber (EPDM); used for the housing of polymeric electrical insulators. EPDM samples with different arrangements of the polymer chains and crystalline degree, promoted by controlled neutron irradiation were studied. Several characterization techniques, as infrared absorption spectroscopy (IR), differential scanning calorimetry (DSC), positron annihilation lifetime spectroscopy (PALS) and dielectric strength (DS) were also used. The relationship between the DS and the degree of movement of polymer chains promoted by electrical forces coming from the electric field applied in a non destructive test as the DMA was successfully established. In fact, a larger empty space in the sample leads to larger areas swept by the polymer chains during bending under the application of the field strength in the dynamic mechanical analysis tests. Therefore, an increase in the capability of movement of charges occurs, corresponding to smaller dielectric strength values. Crystallinity improves the dielectric strength due to the increase in the internal stresses which decreases the capability of movement of the polymer chains and electric carriers by electric forces.

Index Terms - **EPDM, dielectric strength, dynamic mechanical analysis, crystallinity, internal stresses, polymer chains mobility, positron annihilation lifetime spectroscopy, differential thermal analysis**

Manuscript received on 28 September2016, in final form 20 February 2017, accepted 2 March 2017. Corresponding author: O. A. Lambri.

DOI: 10.1109/TDEI.2017.006359

1 INTRODUCTION

One of the most common reasons for using composite polymeric insulators in both transmission and distribution lines is related to the low weight. The weight of a composite polymeric insulator is normally only about 10% of the equivalent porcelain or glass type. Then, composite polymeric insulators enable lighter tower designs or upgraded existing lines. Another important reason is associated with cost reduction, which would include lower cost for transport and construction, for narrower rights of way and for less maintenance [1]. Moreover, composite polymeric insulators exhibit another advantages regarding the glass and ceramic insulators, related to the high mechanical strength to the weight ratio, high vandal damage resistance, low surface energy which allows them maintaining a good hydrophobic surface property in the presence of wet conditions such as fog, dew and rain [2, 3]. Indeed, composite polymeric insulators exhibit superior electrical performances to high voltage insulation system for outdoor power electric devices and apparatus [1–4].

However, leakage current induced on polymer surfaces by contamination buildup and sustained moisture during outdoor service can produce electrical discharges. In fact, dry band arcing at currents as low as 1 to 20 mA may be responsible for surface erosion of non-ceramic insulators. At these currents the relatively stable arc-roots, at localized regions of reduced resistance, are able to inject significant energy into the non-ceramic material. Corona and dry band arcing are very different mechanisms, since corona is a field related phenomenon, while dry band arcing is a leakage current related one. Dry band arcing can only happen once hydrophobicity has been lost, since a hydrophobic surface will have no leakage currents [5, 6].

Electrical discharges can change chemical and morphological structures and cause tracking and erosion, which considerable reduce their mechanical and dielectric strengths. Indeed, the deterioration of the crystalline degree due to the oscillating electric field in composite polymeric insulators in outdoor service was already reported [7]. In addition, ultraviolet irradiation, thermal, acids and corona discharges contribute to accelerate the deterioration of the mechanical and electrical performances [3, 4, 8]. Electric breakdown occurs when the current flowing through the sample increases, leading to its failure and consequently, the applied voltage cannot be stable. The voltage, leading to the material disruption is called breakdown voltage, and the corresponding voltage gradient at failure is the dielectric strength, DS [4, 8]. The understanding of the physical-chemical breakdown mechanisms is not yet complete, but one could distinguish the following processes: intrinsic breakdown, thermal breakdown, gas-discharge dependent breakdown, physical dependent breakdown [4, 6, 8, 9, 10]. Electrical treeing is another mechanism, which may lead to electrical breakdown. Treeing is related to sporadic discharges that are intermittent and not steady like corona discharge. The mechanism of treeing is very similar to electric breakdown, because both start in the regions with the highest and most divergent electrical stresses [6, 8, 11, 12]. In fact, as it can be inferred from above, the electric breakdown phenomenon of insulating materials is a very complex problem due to the large quantity of variables which are involved. Consequently, for instance, empirical expressions have been derived for describing DS as a function of thickness or for DS as a function of time when the insulating material is subjected to corona effect [4]. Therefore, there is today a great need for more research activities to cover numerous aspects pertinent to outdoor insulation as for instance the production and performance of new materials, the understanding of electrical, chemical, and mechanical deterioration mechanisms, the proper dimensioning, design, etc., among others [1].

In order to contribute to the understanding of the electrical breakdown phenomenon, dynamic mechanical analysis, DMA, studies conducted under high electric field, were performed in commercial ethylene-propylene-diene M-class rubber (EPDM) used for the housing of the mechanical resistant core of the polymeric electrical insulators; which are often used either in transmission and distribution lines. EPDM samples with different arrangements of the polymer chains and crystalline degree, promoted by controlled neutron irradiation were studied. Several characterization techniques, as infrared absorption spectroscopy (IR), differential scanning calorimetry (DSC), positron annihilation lifetime spectroscopy (PALS) and dielectric strength (DS) were also used.

The relationship between the DS and the degree of movement of polymer chains promoted by electrical forces coming from the electric field involved in a non destructive test as the DMA under high electric field was established. The formalism of the electric inclusion [13] was applied and the study of the behavior of β coefficient, for the electric case, was carried out.

In contrast to the work in [13], the study of the behavior of β (electric) coefficient as a function of the electrical field is applied to polymeric EPDM matrixes with different arrangement of polymer chains and inclusions (crystallites). The present studied EPDM samples exhibits different both volume fraction and size of crystallites and different degree of empty spaces. Then, in the present work we are studying the overlapping of the internal stresses promoted by both the crystallites and the internal stresses from electrical inclusion caused by the electric field. In addition, the present study of the behavior of the internal stresses is also different to the previously reported results in [6]. Indeed, in [6] the changes in the internal stresses in the EPDM, viewed through the β (non-electric) coefficient; were promoted by the different arrangements of the crystals in the matrix, i.e. different volume fraction and size of crystals.

It should be highlighted that, the study of electrical β coefficient allows determining a value of the degree of area swept by the polymer chain due to the electrical force for a given mesostructure and to relate this value with the dielectric strength. Results here reported, could be useful for helping to the design of new insulating materials with controlled and/or improved dielectric strength behavior.

2 THEORETICAL BACKGROUND

In this Section, the concepts and equations related to the misfit of strain in a polymer for the case of dielectric materials will be shown [13]. The model takes the idea of partitioning the volume of the sample in small elementary cubes in such a way that each partitioned element is composed by a single phase; dipolar or non-polar in the polymer material we are dealing with [13]. Figure 1 summarizes the main concepts to take into account for the case of dielectric materials. It shows a (z,y) plane of the partitioned sample at x = v, where the size of the partitioned matrix, over each axis, was chosen equal to lo_p.

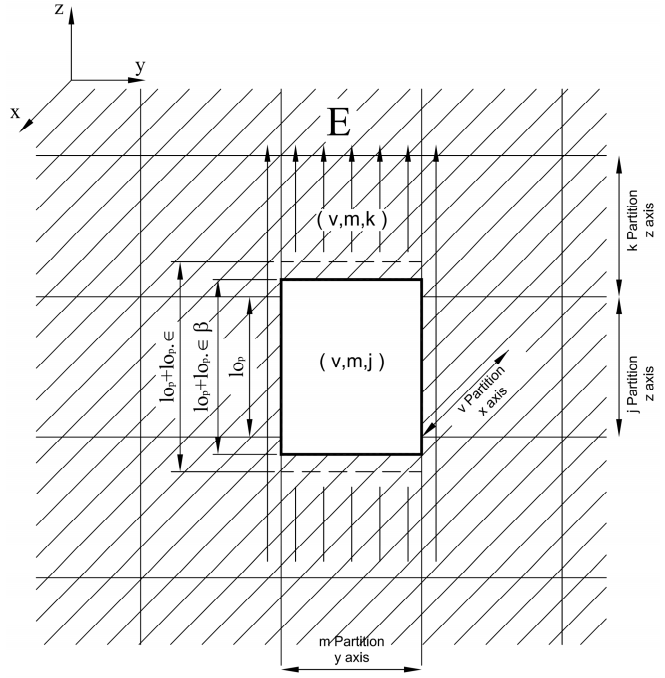

Figure 1. Equilibrium position of the boundary between the dipolar inclusion and the matrix, after location of the stretched inclusion into the matrix hole and release of its constriction. See explanation in the text.

The model now starts with the following considerations:

a) The volume element corresponding to a dipolar phase, located at (v,m,j) of the whole partitioned matrix, which is plotted by means of full fine lines in Figure 1, is cut and removed out of the matrix; leading to a cubic hole of edge lo_p.

b) An electric field is applied to this extracted dipolar zone, then it stretches from lo_p to $lo_p + \in lo_p$, with $0 \leq \in \leq 1$, see broken lines in Figure 1. It is easy to recognize that the mismatch parameter $\in$ is the strain misfit promoted thorough an electrostrictive phenomenon. Indeed, the application of the electric field give rise to the appearance of an inclusion of larger size into the matrix, plotted by means of broken lines.

c) The inclusion of size $lo_p + \in lo_p$, with $0 \leq \in \leq 1$, plotted by means of broken lines, will be firstly compressed to fit into the hole of the matrix and subsequently placed in.

d) The inclusion is mechanically released and then the boundaries of the hole, in the z-axis, displace to a position $lo_p + \beta \in lo_p$, with $0 \leq \beta \leq 1$, where the equilibrium of stresses is achieved. The wide lines in Figure 1, represent this state.

Therefore, by means of the above described procedure, the elastic misfit promoted by an electric dipole when an electric field is applied, can be studied now using the mathematical formalism of the inclusions theory. In fact, in the present study β is the misfit coefficient, which is related to the matrix strain caused by the stretching of the dipole when the electric field appears, and it takes the form [6, 13]

$$\beta^z = \frac{1}{1+\left(\frac{M_m}{M_i}\right)\cdot\left(\frac{fr_i^z}{fr_m^z}\right)} \quad (1)$$

where M is the Young modulus, f the volume fraction and the sub-indexes m and i correspond to the matrix free of electrostrictive effects and to the inclusion (stretched dipole) elements, respectively. The supra-index "z" indicates that the direction for the study of the problem is the z axis.

By working mathematically, it was shown that β coefficient can be calculated, despite of unknowing the elastic modulus of the dipolar zone (M_i), from [13]

$$\beta = fr_m \frac{M}{M_m} \quad (2)$$

where M refers to the Young modulus of the whole material when electrostictive effects appear, i.e. the material containing the matrix and the dipolar inclusions stressed. Indeed, equation (2) makes possible to calculate the misfit coefficient in dielectric materials, or two-phase polymers, knowing the elastic modulus of the matrix, free of electrostrictive effects, its volume fraction and the elastic modulus of the whole material, when the electrostrictive effects appear. See for more details [6, 13–15].

3 EXPERIMENTAL

3.1 SAMPLES

Samples were taken from commercial EPDM used as housing of non-ceramic electrical insulators (Avator of Sitece Electrical Industries, Buenos Aires, Argentina), which are employed in outdoor transmission lines of 66 kV. EPDM composition was determined by means of IR spectroscopy, following directions of ASTM D 3900 standard [16]. The nominal molar composition of the rubber was 65% ethylene – 32% propylene and 3% ethylidene-norborene. EPDM used in the present work was reinforced with ceramic particles of Bayerite (alumina-trihydrate, ATH) in a proportion of 44 wt%, as it is usual for electrical applications in order to improve the flashover resistance [2].

3.2 NEUTRON IRRADIATION

Neutron irradiations were performed at the RA-6 nuclear reactor of the National Atomic Energy Commission of Argentina, which was operated at 400 kW and 200 kW. Samples irradiated at 400 kW will be called hereafter samples

of A-type and samples irradiated at 200 kW will be called hereafter samples of B-type. All samples were irradiated with bismuth and cadmium filters at room temperature in air. Table 1 shows the details of the used samples in the present work.

Table 1. Sample characteristics and denomination.

Reactor Power	Neutron Flux (n/cm²s) Thermal / Fast	Dose (Gy)				
		82	**415**	**830**	**4150**	**8300**
400 kW	$1.7x10^8$ / $5.5x10^8$	A1	A2	A3	A4	A5
200 kW	$8.5x10^7$ / $2.75x10^8$	B1	B2	B3	B4	B5

Dummy specimens of EPDM, which were irradiated together with the samples, were studied by means of IR in order to check if oxidation was promoted during the neutron irradiation. IR studies could not reveal the appearance of oxidation in all the irradiated samples.

In order to obtain different crystalline volume fraction and size of crystals, without oxidation of the samples and with crystallites homogeneously distributed into the matrix, neutron irradiation, among different procedures for promoting chemicrystallization, e.g. thermal oxidation, electron irradiation, etc.; was chosen. Oxidation processes by thermal annealing can be an easy mode of promoting chemicrystallization [17]. Nevertheless, the oxidation leads to changes in the polymer matrix which can modify its electrical behavior under high electric fields [4, 8]. Moreover, oxidation treatments can lead to an inner gradient of oxidation in the sample, giving rise to inhomogeneous distribution of crystals. In addition, electron irradiation depends on the incident energy for trespassing the sample, but usually the cascade of damage is larger at the front near of the incident beam. In contrast, the neutrons can penetrate into the sample and the atom without hindrance. When they collide with nuclei they are either, absorbed by them or recoil from them. In elastic neutron scattering in substances containing a large number of hydrogen atoms, the energy of incident neutrons is halved on an average, being transferred partially to recoil protons [18,19]. Then, a more homogeneous distribution into the matrix of the chemicrystallization process should be obtained.

3.3 MEASUREMENTS

IR studies were carried out in a Shimadzu Prestige 21, FTIR spectrometer, with an attenuated total reflectance (ATR) accessory. 40 scans per spectrum, in the wavenumber range of 4000 - 400 cm^{-1} with a resolution of 4 cm^{-1}, were used for each studied sample.

DSC measurements were performed in a Perkin-Elmer Jade DSC equipment with aluminum crucibles at a heating rate of 10K/min. Measurements were performed under helium at atmospheric pressure. The explored temperature interval was from 173 K up to 368 K.

DTA measurements were performed in a conventional calorimetric equipment employing stainless steel crucibles under argon at atmospheric pressure, from 173 K up to 368 K. The used heating rate, controlled by a Lake Shore DRC-91C controller, was of 10 K/min.

PALS measurements were performed at 300 K by a conventional fast–fast timing coincidence system with a resolution (full width at half maximum) of 240 ps. As positron source a ^{22}NaCl source of about 15 μCi evaporated onto a thin Kapton foil was used. The measuring time for all the neutron irradiated samples was similar. All lifetime spectra were analyzed in three components after subtracting the source contribution. The LT_92_3 program [20] to fit the spectra with a continuous distribution of positron lifetimes for the long lifetime τ_3 was used. In the present work, we are interested in the evolution of the average of the free volume; so, we have particularly analyzed the parameters of the long component, lifetime and intensity, which are related to the free volume present in the sample. Indeed, following the common interpretation of PALS measurements in polymers, the long-lifetime component (τ_3) is associated with ortho-Ps annihilation by pick-off processes. From that, the mean size of the holes forming the free volume can be roughly estimated by means of the Eldrup model [21]. In such a model, the ortho-Ps lifetime, τ_3, as a function of the free-volume radius, R, is given by,

$$\tau_3 = 0.5 \left[1 - \frac{R}{R_0} + \frac{1}{2\pi} \sin \left(\frac{2\pi R}{R_0} \right) \right]^{-1} \quad (3)$$

where, $R_0 = R + \Delta R$ and τ_3 is given in nanoseconds. ΔR is an empirical parameter whose best-value was obtained by fitting all known data and it is 1.656 Å [22]. The mean free volume hole size, V_f, assuming a spherical form for the holes, may be estimated by means of the following equation:

$$V_f = \left(\frac{4\pi}{3} \right) R^3 \quad (4)$$

The experimental data of a positron lifetime experiment in polymers are usually the convolution of three exponentials decays (i.e. three different lifetimes) with the resolution function of the spectrometer. Each lifetime corresponds to the inverse of the average annihilation rate of a positron in that state: the shortest and the intermediate lifetimes have contributions from the singlet para-positronium ($\tau_1 \approx 0.12$ ns) and positron annihilation in different molecule species. On the other hand, the longest lifetime ($\tau_3 \geq 1$ ns) is due to ortho-Ps localized in free volume holes. In this analysis, the τ_3 component is used to determine the mean free-volume hole size. The relative intensity corresponding to this lifetime, I_3, contains information related to the number of the free-volume holes from which positronium annihilates. In this sense, combining the number (I_3) and size (τ_3) of free volume holes an estimation of the free volume fraction (f) could be extracted [23]:

$$f = A V_f \, I_3 \quad (5)$$

where A is a proportionality constant, which can be determined by calibrating with other physical parameters [24,

25]. However, it is difficult to know the value of A for many polymers. So, Li et al has defined an apparent fractional free volume (AFFV) by the following equation [26]:

$$f_{app} = V_f \; I_3 \qquad (6)$$

DS measurements were performed immersing the EPDM samples into a dehydrated soybean oil bath thermalized at (300.0 ± 0.3) K. The cell for the bath is cubic with a volume of 350 cm^3 and it was constructed in atactic poly-methyl methacrylate (PMMA). EPDM samples for dielectric strength tests were parallelepiped shaped samples of 15 mm x 15 mm x 4 mm. Dimensions were determined with an error of around 0.02 mm. Electrodes were cylinders of stainless steel with 2 mm diameter, with flat base. Samples were placed between the two electrodes, with a gap of 4 mm, which were in soft contact with the surface of the sample. The equipment for measuring DS has an automatic rising voltage at 2 kV/s. It also has an automatic detection system for the cut of the run-up in voltage by measuring the derivative of the current increase.

The voltage and current behaviors in the primary coil of the transformer were also monitored. Details for the DS equipment were already reported in [6]. Prior to DS measurements, the surfaces of the sample were carefully cleaned and washed in bidistilled water and subsequently dried in air at 300 K during 12 hours. If the cleaning of the sample is avoided arcs may appear on the surface of the sample. Plotted values of DS in Figure 4 are the result of 8 measurements performed in two different samples, four measurements by sample. In each sample four positions for locating the electrodes were chosen in order to describe one square of 5 mm edge, see [6] for more details.

DMA tests, loss tangent (damping or internal friction), tan(ϕ), and dynamic shear modulus, G', were measured as a function of the applied electrical field, E, in a mechanical spectrometer working in torsion at temperature of 318 K (± 0.3 K), in air. The resonance frequency was around 20 Hz. Damping was determined by measuring the relative half width of the resonance peak for a specimen driven into forced vibration using equation (7) [13]:

$$\tan(\phi) = \frac{\omega_2 - \omega_1}{\omega_0} \qquad (7)$$

where ω_0 is the resonance frequency, and ω_1 and ω_2 are the frequencies at which the amplitude of oscillation has fallen to $1/\sqrt{2}$ of the maximum value. The errors of tan(ϕ) and G', being proportional to the squared oscillating frequency, are less than 1%. The maximum oscillating strain on the surface of the sample was $2x10^{-4}$.

The electric field, E, was produced by two electrodes placed at the sample position, lying in parallel direction to the torsion axis of the spectrometer, i.e. the resulting electric field is perpendicular to the torsion axis. Electrodes were connected to a variable DC high voltage power supply, giving rise to E values up to 735 kV/m, at the sample location. For more details see Ref. [13, 27].

4 RESULTS AND DISCUSSION

Figure 2 shows the behavior of the enthalpies related to the melting of the crystalline zones (right axis) and the crystallites concentration (left axis), as a function of the irradiation dose for both A- and B-type samples; determined from calorimetric studies.

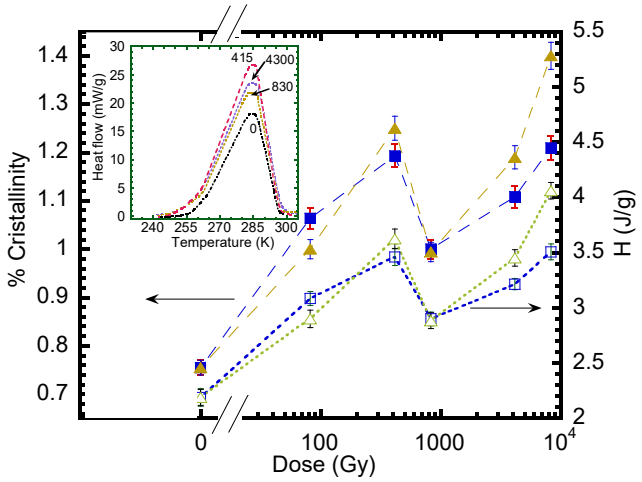

Figure 2. Percentage of crystallinity (full symbols) and melting enthalpy (empty symbols) for non-irradiated and irradiated EPDM samples. A-type samples: Squares. B-type samples: Triangles. Dashed lines are a guide for the eyes. Inset: DSC thermograms for non-irradiated sample and some irradiated A-type EPDM samples.

A-type samples were studied by means of DSC and B samples were studied by means of DTA. The real value of the melting enthalpy from DTA was calculated by relating the area of the measured reaction with the area and energy from DSC studies. An excellent correspondence among the values of DSC and DTA thermograms for all the non-irradiated and irradiated samples was found.

The percentage of crystallinity was determined by considering the relation of the measured enthalpy to the melting enthalpy of crystallites in a 100% crystalline polyethylene (290 J/g) [28]. Inset in the Figure shows the endothermic reaction related to the melting of crystalline zones for A-type samples at around 285 K, measured from DSC studies; where only some doses were included for clarity. The melting temperature was in agreement with previous reported works [6, 14, 15, 29, 30].

As it can be seen from the figure, the evolution of both the melting enthalpy and the volume fraction of crystals do not exhibit a monotonous behavior, which is in agreement with previous works [6, 14, 15, 29, 30]. The enthalpy, and consequently, the volume fraction increase up to 415 Gy and then decrease at 830 Gy. Subsequently, the volume fraction and enthalpy re-increase as the dose increases. In fact, the volume fraction and size of the crystallites in EPDM can be modified depending on the irradiation dose and flux [29, 30].

The modification of the size of crystallites was explained considering the competition of two physical effects during neutron irradiation: (i) the growing of the small crystals for decreasing the interface energy through a chemicrystallization

process and (ii) the deterioration of crystals as a result of neutron irradiation [6, 30]. As it can be easily inferred, there exist a relationship between the melting enthalpy and the size of crystals. In fact, an increase in the melting enthalpy can be related to the increase in size of crystal in such a way that larger crystals are thermodynamically more stables and then more energy is required for melting [31-34].

Chemicrystallization is produced by the piling up of nearby located cut polymer chains of the amorphous matrix. Neutron irradiation produces chain scissions, the scission products having less restricted mobility. Disentanglement of such fragments allows them to crystallize into imperfect, low-melting point crystals, increasing the overall crystalline content [17, 29-32, 35].

In the other hand, it is appropriate to mention here that, the PALS and DS curves for A-type samples were already reported in a previous work [6]. However, these results are re-plotted here for improving the clarity of the discussion of the present results.

Figure 3 shows the behavior of the hole free volume (V_f, full symbols), and the apparent fractional free volume, AFFV (V_f, x I_3, empty symbols), determined from PALS (see Section 3.3) for the non-irradiated and irradiated A- and B-type of samples, as a function of irradiation dose. For A-type samples the empty space in the sample, AFFV, increases monotonously as the irradiation dose increases.

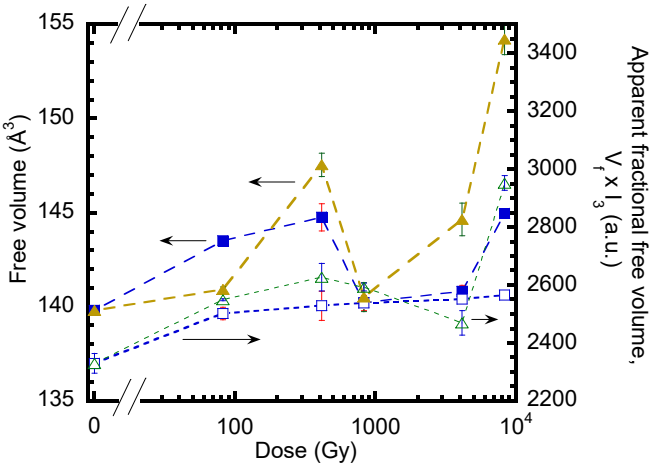

Figure 3. Hole free volume (full symbols) and apparent fractional free volume (empty symbols) for non-irradiated and irradiated EPDM samples, determined from PALS at room temperature. A-type samples: Squares. B-type samples: Triangles. Dashed lines are a guide for the eyes.

The increase in AFFV was already explained by the increase in the volume fraction of the crystalline zones promoted by neutron impacts through a chemicrystallization process [14, 15]. Indeed, the length of the polymer chains per unit area, within the newly formed crystalline zone, is shorter than when the same zone is amorphous, leading to a less dense matrix. So, the AFFV (empty space) increases with the increase in the volume fraction of the new crystallites [15]. In contrast, for B-type samples the AFFV increases up to 415 Gy, followed by a decrease up to 4300 Gy and a further increase at 8300 Gy.

The non monotonous behavior of AFFV as a function of the irradiation dose for B-type samples can be explained by considering that during neutron irradiation, the promotion of new crystals by chemicrystallization and the chain scission are occurring overlapped. It leads to different arrangements of the polymer chains as a function of both the irradiation dose and neutron flux which can reduce the AFFV at some doses. In fact, the goal of studying neutron irradiated EPDM is that different arrangements of the mesostructure can be obtained depending either of the dose and neutron flux [6, 14, 29, 30].

The behavior of the hole free volume as a function of the irradiation dose for both types of samples, is also shown in Figure 3. A similar trend between the two kinds of samples can be observed. However, the hole free volume measured at 8300 Gy for the B sample is the largest one.

It was earlier reported that the size of the holes into the polymer matrix (hole free volume, V_f), is controlled by the size of the crystals. A larger size of the crystals leads to larger size in the hole free volume and vice-versa [14, 15]. This correspondence was explained by means of the inclusion theory when the inclusion is smaller than the size of the hole into the matrix [15]. Then, we can deduce from PALS studies the following evolution according to dose, for both kinds of samples: The size of holes increases up to an irradiation dose of 415 Gy, and it decreases to a value close to the non-irradiated sample for an irradiation dose of 830 Gy. Subsequently, for higher irradiation doses the free volume increases again, reaching its highest value for a dose of 8300 Gy. In addition, the largest value of the size of holes was measured for B-type sample irradiated at 8300 Gy.

It should be stressed that, there exists a good correspondence between the behavior of the hole free volume (Figure 3) and the melting enthalpy of crystals (see Figure 2), as a function of the irradiation dose. In fact, as said before, larger crystals are thermodynamically more stable than smaller ones and then, they require more energy to melting, which is in agreement with the classical theory of nucleation and growth [33, 34, 36, 37].

Figure 4 shows the behavior of DS for non-irradiated and irradiated A- and B-type samples. As it can be seen from the Figure, the values of DS for A-type sample decrease as the dose increases. Moreover, it is interesting to note that a marked step-down at 830 Gy happens [6]. For B-type samples, the DS values are smaller than for A-samples up to dose smaller than 4150 Gy. In addition, marked steps-down were measured at 830 Gy and 8300 Gy.

Figure 5 shows the behavior of DS as a function of the empty space (AFFV) for both kinds of samples. For A- type samples, which exhibit a monotonous increase of AFFV as the dose increases, the good correspondence is clear, see squares in the Figure.

Despite, that AFFV for B-samples does not behave monotonously with the irradiation dose, an excellent agreement with previously reported data for A-samples was found. In addition, for 830 Gy, where the crystallinity is destroyed in both type of samples, and for 8300 Gy for B-type of samples, the corresponding points move aside the curves.

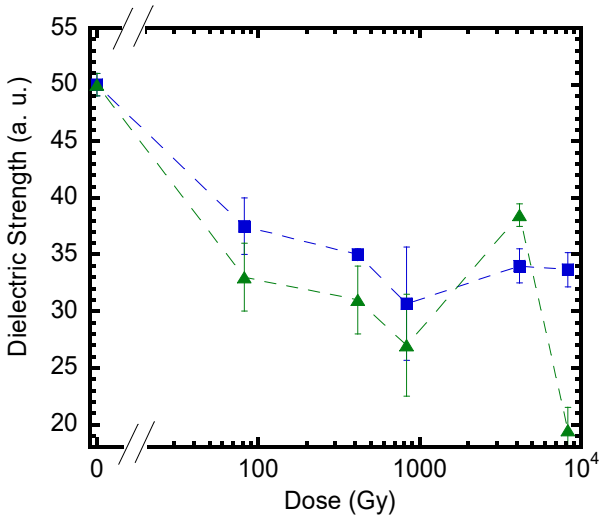

Figure 4. Dielectric strength in arbitrary units measured in non-irradiated and irradiated EPDM samples. A-type samples: Squares. B-type samples: Triangles. Dashed lines are a guide for the eyes.

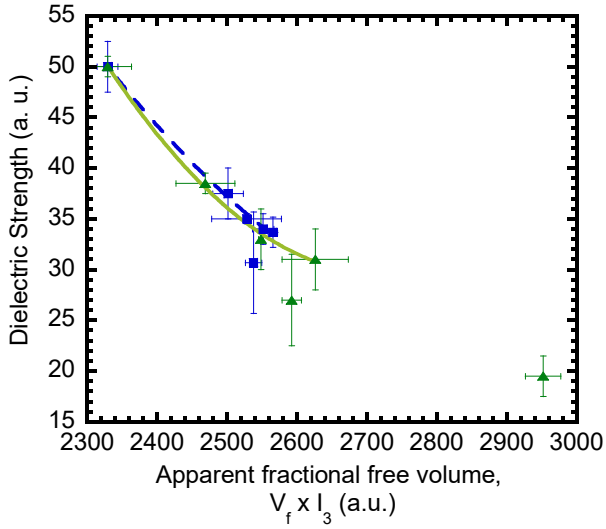

Figure 5. Dielectric strength as a function of the apparent fractional free volume. A-type samples: Squares. B-type samples: Triangles. Lines represent the fitted 2nd degree polynomial. In the fitted curves the point at 830 Gy is not included for both type of samples. For B-type samples the point at 8300 Gy is neither included, see explanation in the text.

Moreover, if we remove the values corresponding to a dose of 830 Gy for both type of samples and the value at 8300 Gy for B-type of samples, the correlation factor of the fitting to a square polynomial of the experimental data, increases appreciably; r = 0.998 and 0.999, for A- and B-type samples, respectively. In fact, as it was previously reported, when crystalline zones are promoted into the matrix in semi-crystalline EPDM and the internal stresses increase, DS decreases as the empty space (AFFV) into the sample increases, owing to the movement of the polymer chains. This movement is mainly controlled by the empty space into the sample, since the entanglement of chains leads to a collective movement of them where no preferable and isolated bends occur. However, when the internal stresses acting at the polymer chains decrease, there appear local zones where the polymer chains start the bend, once the electrical forces are larger than the line tension [6].

Therefore, charges/electric dipoles come from the curing process of the rubber, electric carriers injected from the electrodes, ions from the corona effect, etc. placed inside or adjacent to the polymer chains have a mobility, for sweeping distances at mesoscopic scale, that is strongly dependent on the mobility of the polymer chains [6]. Then, it is clear that a good relationship between the dielectric strength and the empty space of the sample (AFFV) can be established, independently of how larger be the empty space (see Figure 3), but the degree of crystallinity is another variable to be considered.

Consequently, in order to explore the overlap effects among the internal stresses promoted by the crystalline zones, the empty space and the electrical forces acting on charges or polar molecules adjacent or embedded at the polymer chains, DMA studies conducted under high electric field were performed.

Figure 6 shows the behavior of the ratio (G'(E)/G'(E=0)) between values of the dynamic modulus measured at each electric field, G'(E), and the modulus value measured at nil field, G' (E=0), as a function of the electric field strength; for non-irradiated and irradiated samples of Table 1. This ratio was chosen in order to eliminate the error contribution to the modulus from the shape factor of the sample (around some percents), due to the proportionality that exists between the modulus and the square oscillating frequency; such as $G'(E)/G'(E=0) = f^2(E)/f^2(E=0)$. Indeed, the ratio in square frequencies will be studied due to the squared frequency can be measured with an accuracy better than around 0.1%.

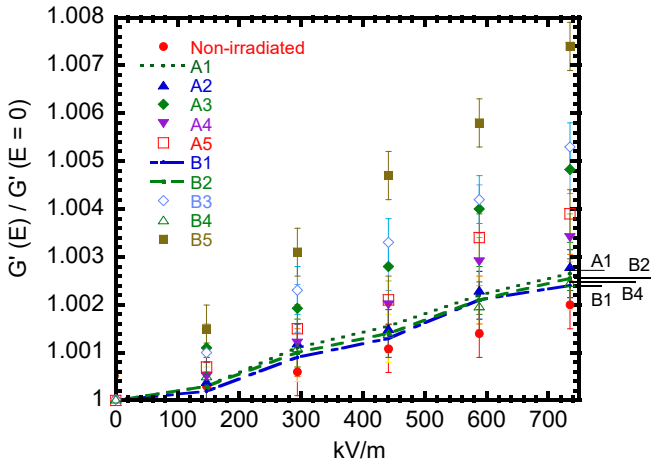

Figure 6. Ratio between the dynamic elastic modulus $G'(E)/G'(E=0) = f^2(E)/f^2(E=0)$ as a function of the electric field strength "in situ" in the DMA tests at room temperature for non-irradiated and irradiated EPDM samples of Table 1.

Curves for samples A1, B1 and B2 are plotted by means of broken lines for the sake of clarity. These curves are lying in the zone between A4 (inverted triangles) and B4 (open triangles) samples. Besides, for these samples the values of the ratio G'(E=734 kV/m)/G'(E=0), at the maximum field strength, are indicated by labeled horizontal lines. In addition, the values of G' at room temperature and nil electric field are in agreement with previous reported works [6, 30].

The increase in the elastic modulus as the electric field increases can be explained by means of the electric-inclusion formalism recently reported in [13], see Section 2. Indeed, the increase in the electric field promotes the stretching of dipoles (polar groups) along the direction of the electric field giving rise to the appearance of an inclusion [13]. The increase in the electric field leads to higher modulus in the inclusion due to the increase in the stretching of the dipoles, until saturation. The orientation contribution of the dipoles could contribute also to the increase in the modulus. An increase in the electric field promotes a strong pinning of the oriented dipoles along the field direction, so a larger anchorage of the dipoles could lead to higher torsion modulus of the inclusions, as the field increases [13]. Consequently, the increase in the moduli of the inclusions, leads to an increase in the modulus of the whole matrix, as it is well known in the mechanical properties of composite and two-phase materials [13, 38-40].

The slope of curves increases as the empty space (AFFV) of samples increases (see Figure 3, right axis). For instance, the increase in slope is clear for B5 sample (8300 Gy), which exhibit the highest value of empty space, see squares in Figure 6. However, for samples irradiated at 830 Gy of both types, A (full diamonds) and B (empty diamonds), which have both, the same crystalline volume fraction (small) and free hole volume, the slopes of the ratio G'(E)/G'(E=0) vs. E are the higher ones except for B-type sample irradiated at 8300 Gy.

In another light, the behavior of tan(ϕ) curves as a function of the applied electric field for the corresponding samples shown in Figure 6 follow the usual trend earlier reported for DMA experiments conducted under high electrical field [13, 27]. In fact, the higher the increase of moduli curves as the field strength increases, the higher the decrease for tan(ϕ) curves as the field strength increases. This behavior is in agreement with the above exposed regarding the development of internal stress in the polymer matrix promoted by the electric field.

The increase in internal stresses in the polymer matrix acts as obstacles which difficult the movement of the polymer chains leading both to a decrease in the damping values and to an increase in the modulus values. Moreover, the values of tan (ϕ) at room temperature and nil electric field are in agreement with previous reported works [13, 30].

It should be highlighted that at mesoscopic level in EPDM a clear view of the problem of the superposition effects of the internal stresses that come from the crystalline volume fraction, size of crystals, empty space and the electric forces promoted by an electric field; can be done for studying the behavior of β coefficient, from the electric inclusion formalism, as a function of the electric field strength. In fact, Figure 7 shows the calculated curves of β, by means of equation (2), for the curves of moduli and volume fraction shown in Figure 6 and Figure 2, respectively. The same criterion for symbols than in Figure 6 was used for clarity.

The curves of β reveal the changes in the internal stresses due to the application of the electric field for the different crystalline states (i.e. volume fraction and size of crystals) and

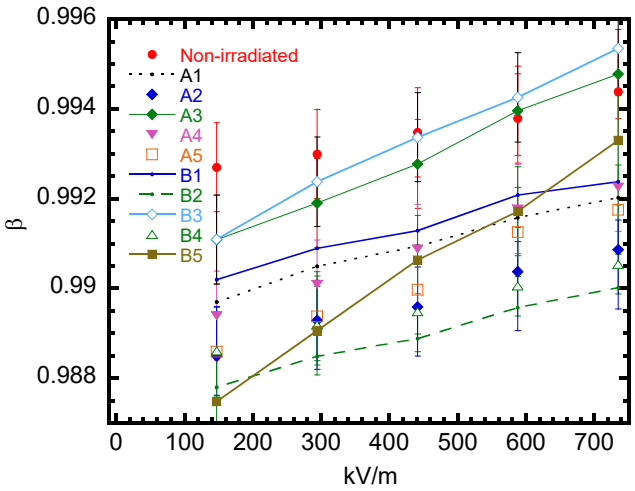

Figure 7. Electric misfit coefficient β (calculated from equation. (2)) as a function of the electric field strength "in situ" in the DMA tests at room temperature for non-irradiated and irradiated EPDM samples of Table 1. Symbols are as in Figure 6. Full lines are a guide for the eyes.

empty spaces in the samples. For this reason, β is only defined from 142 kV/m upwards, as it was earlier described in Section 2. Indeed, the behavior of β coefficient is different depending whether the source of internal stresses is promoted by a change in volume fraction of inclusions, as in the case of crystal growth, or by a change in the modulus of the inclusion, as in the case of dipoles under an electric field. These two cases were carefully analyzed in a previous work [13].

The initial decrease of β values at the smallest field strength among the different kinds of samples is mainly related to the change in the crystals size. In fact, larger crystals lead to smaller β coefficient, because the internal stresses into the matrix have increased due to accommodation of the strain misfit. Moreover, the trend exhibited as a function of the crystal size for the A-type of samples at the smallest field, is in agreement with the already reported work focused on the study of the internal stresses during the crystal growth [6].

In contrast, the increase in β values as the field increases, indicates that the increase in the strain misfit is mainly accommodated by the matrix, i.e., $\beta \rightarrow 1$ leads to $lop + lop\in\beta \rightarrow lop + lop\in$ (see Figure 1). The increase of the electric field, leads to an increase in the modulus of the inclusion (see Figures 1 and 6); forcing the matrix to accommodate higher strain misfit, so leading to an increase of β [13]. In other words, the polymer chains in the polymer matrix, pushed by the electric force, sweep larger distances as the field increases leading to a β increase, see Figure 1. In addition, as larger is the empty space in the matrix, larger is the slope of β (called hereafter Sβ) and vice-versa, see Figure 8, so an increase in the swept area by the polymer chains have taken place (see Figure 1), i.e. the distance swept by charges in movement has increased. In fact, the movement of the charges embedded in the chain entanglement, over distances at mesoscopic level is always dependent on the mobility degree of the entanglement of the polymer chains in the matrix, as it could be expected [6]. Molecular chains under electrical forces during their movement must overcome potential energy barriers from the

matrix. An increase both in the empty space of the matrix and β values is indicating that the gap between the rest state and the saddle point of the energy configuration has decreased, leading to an increase in the mobility of the chains and then an increase in the mobility of the charges.

In contrast, for sample B3 that exhibits a deterioration of the crystalline state by irradiation, the slope in β increases markedly (Figure 8), even if the empty space decreases slowly at this dose.

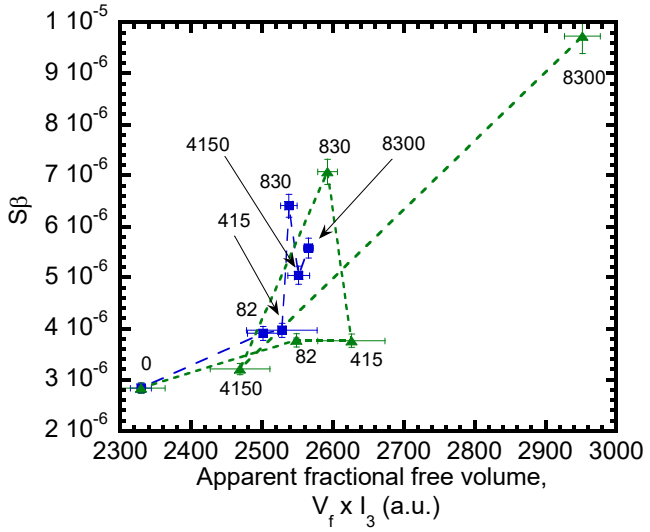

Figure 8. The slope of the curves of β as a function of the strength field (Figure 7), Sβ, as a function of the apparent fractional free volume. A-type samples: Squares. B-type samples: Triangles. Dashed lines are a guide for the eyes.

It is interesting to highlight the behavior of β curves as a function of the field strength for samples A3, B3 and B5, Figure 7. Indeed, A3 and B3 have the smallest crystalline volume fractions among the irradiated samples and they exhibit the highest Sβ except for B5 sample. In addition, the values of β for E = 735 kV/m are even higher than the ones for the non-irradiated sample. In contrast, B5 sample exhibits the largest empty space in the sample, so the Sβ is the highest in Figure 7 and 8, in agreement with the above exposed.

However, B5 has also the largest size and volume fraction of crystals, and the β value at the highest strength field is even smaller than the corresponding one to the non-irradiated sample. Therefore, it should be emphasized that the behavior of β shown in Figure 7 is a consequence of the overlapping of all contributions to the internal stresses in EPDM, i.e. crystallinity, empty space and electrical forces.

Figure 9 shows the behavior of DS as a function of Sβ for non-irradiated and all irradiated and A- and B-type samples. As it can be seen from the Figure, an increase in Sβ leads to a decrease in DS values. In fact, as larger are the areas swept for the polymer chains under the application of the electric field, larger is the contribution of charges in collective movement in the sample.

Therefore, it is reasonable that an easier collective movement of charges lead to a decrease in the DS, which is in agreement with the above exposed and previous works [4, 6, 8].

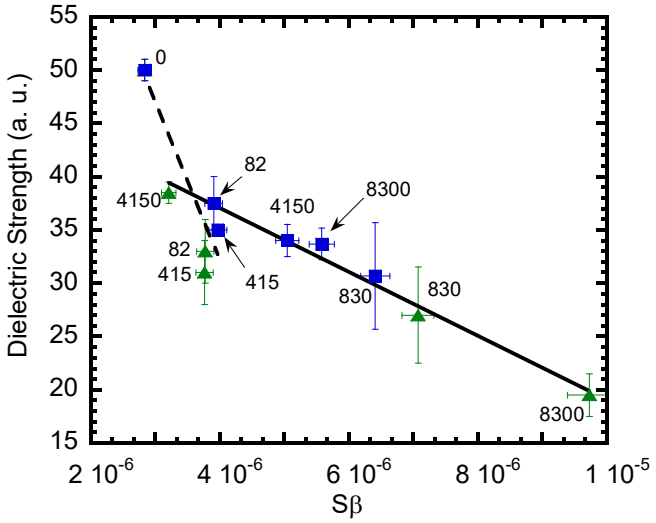

Figure 9. Dielectric strength as a function of the slope of the curves of β as a function of the strength field (Figure 7), Sβ. A-type samples: Squares. B-type samples: Triangles. Dashed line is the fitted straightline for samples irradiated at doses smaller than 830 Gy. Full line is the fitted straightline for samples irradiated from 830 Gy upwards, see explanation in the text.

Despite that a simple relationship between DS and Sβ could not be found, two linear stages could be identified, notwithstanding the mismatch of the fitted line (see broken line) regarding to some error bandwidths. In fact, the first linear stage (broken line) corresponds to samples prior to the deterioration of the crystalline state at 830 Gy. In contrast, the second linear stage (full line) corresponds for samples after re-increase both of the volume fraction and the size of crystals. The two stages for describing the law of DS against the Sβ could be controlled by the different arrangement of crystalline zones (volume fraction and size) and empty space in the polymer matrix after the re-construction of the crystal growth by chemicrystallization.

It should be highlighted that Figure 9 reveals the correspondence between the magnitude of the swept area by the polymer chains from a non-destructive test and the electrical breakdown phenomenon. The use of the behavior of the β coefficient (electric) and its slope as a function of the field strength from DMA studies conducted under high electric field could be useful for the design of polymer chemical formulations with improved dielectric strength response, by controlling for instance crystallinity and empty space in the polymer. In fact, a relative measure of the distance evolved by the electric carrier under electric strength can be obtained from β for different mesoscopic polymer arrangement, so, it could be useful for the design of polymer formulations and their tests.

In another light, the above discussion was focused on charges at dipoles in agreement with the electric inclusion model described in Section 2. However, it could also be applied to isolated charges. In fact, isolated charges can push the polymer chains promoting a state of stresses and strains in the continuous formalism similar to one occurring at the interface between the inclusion and the matrix, see Figure 1. Nevertheless, for isolated charges the elastic problem loss the

symmetry of the inclusion theory, but from a local point of view of the interface, the problem of the promotion of internal stresses and the resulting strains could be assumed as similar and then, it could be studied through β coefficient.

5 CONCLUSION

The formalism of the electric inclusion trough the study of β electric-coefficient was applied successfully to EPDM samples exhibiting different arrangement of the polymer chains at mesoscopic level, i.e. crystallites concentration, size of crystallites and empty space; promoted by means of controlled neutron irradiation. The behavior of β electric-coefficient as a function of the field strength from dynamic mechanical analysis tests was determined to be appropriate for describing the behavior of the internal stresses as a function of crystallinity, empty space and electric forces in the polymer and their relation to the dielectric strength.

The relationship between the dielectric strength and the degree of movement of polymer chains promoted by electrical forces coming from the electric field involved in a non-destructive test as the dynamic mechanical analysis was established. A larger empty space leads to larger areas swept by the polymer chains during bending under the application of the field strength in the dynamic mechanical analysis tests. Therefore, an increase in the capability of movement of charges occurs, corresponding to smaller dielectric strength values. Crystallinity improves the dielectric strength due to the increase in the internal stresses which decreases the capability of movement of the polymer chains and electric carriers by electric forces.

It should be highlighted that, the study of β electric-coefficient allows determining a value of the degree of area swept by the polymer chain due to the electrical force for a given mesostructure and to relate this value with the dielectric strength. Then, the dynamic mechanical analysis studies conducted under high electric field could be used as a useful tool for helping to design new insulating materials, with controlled and/or improved dielectric strength behavior, and their testing.

As a consequence of the studied case, which involves samples with different arrangement of empty space and mechanical and electrical inclusions, the present study give the general lineament for being applied either in crystalline and non-crystalline polymers. The strength of the external field being the variable to be changed which would depend on the kind of the polymer to be tested.

ACKNOWLEDGMENT

This work was partially supported by the CONICET-PIP No. 179CO, the PID-UNR ING 450 (2014-2017) and the Cooperation Agreement between the Universidad del País Vasco/Euskal Herriko Unibertsitatea and the Universidad Nacional de Rosario, Res 3243/2015. A.O.L wishes to say thanks to his friend the Rev. P. Ignacio Peries for everything.

REFERENCES

[1] S. M. Gubanski, "Modern outdoor insulation - concerns and challenges", IEEE Electr. Insul. Mag., Vol. 21, No. 6, pp. 5–1, 2005.

[2] R. Hackam, "Outdoor HV composite polymeric insulators", IEEE Trans. Dielectr. Electr. Insul., Vol. 6, No. 5, pp. 557–585, 1999.

[3] S. Kumagai, *Fundamental Research on Polymeric Materials Used in Outdoor High Voltage Insulation*, Akita University, Japan, 2000.

[4] W. W. Pendleton, *Encyclopedia of Materials Science and Engineering*, Pergamon Press, Oxford, 1986.

[5] J. P. Reynders, I. R. Jandrell and S. M. Reynders, "Review of aging and recovery of silicone rubber insulation for outdoor use", IEEE Trans. Dielectr. Electr. Insul., Vol. 6, No. 5, pp. 620–631, 1999.

[6] O. A. Lambri, F. Tarditti, J. A. Cano, G. I. Zelada, J. A. García, D. Merida Sanz, F. Plazaola Muguruza, C. E. Boschetti and G. E. Martinez Delfa, "Influence of empty space and internal stresses on dielectric strength in two-phase polymer", IEEE Trans. Dielectr. Electr. Insul., Vol. 20, No. 5, pp. 1869–1881, 2013.

[7] P. Sorichetti, C. Matteo, O. A. Lambri, G. Manguzzi, L. M. Salvatierra and O. Herrero, "Structural Changes in EPDM Subjected to Ageing in High Voltage Transmission Lines", IEEE Trans. Dielectr. Electr. Insul., Vol. 14, No. 5, pp. 1170–1182, 2007.

[8] J. Ulanski and M. Kryszewski, *Polymers, Electrical and Electronic Properties,* Encyclopedia Appl. Phys., Ed. Trigg G. VCH Publishers. Inc., New York, pp. 497, 1996.

[9] A. J. Phillips, D. J. Childs and H. M. Schneider, "Water drop corona effects on full-scale 500 kV non-ceramic insulators", IEEE Trans. Power Deliv., Vol. 14, No. 1, pp. 258–265, 1999.

[10] J. Kuang and S. A. Boggs, "Thermal-electric field distribution around a defect in polyethylene", IEEE Trans. Power Deliv., Vol. 13, No. 1, pp. 23–27, 1998.

[11] N. H. Malik, A. A. Al-Abdullah, A. A. Al-Arainy and M. I. Qureshi, "Factors influencing electrical treeing in XLPE insulation", Eur. Trans. Electr., Power, Vol. 16, No. 2, pp. 205–218, 2006.

[12] C. Mayoux, "Studies on the aging processes of polymers in electrical systems", Die Angew. Makromol. Chemie, Vol. 261–262, No. 1, pp. 143–156, 1998.

[13] O. A. Lambri, R. R. Mocellini, F. Tarditti, F. G. Bonifacich, D. Gargicevich, G. I. Zelada and C. E. Boschetti, "Internal stresses in the electrostriction phenomenon viewed through dynamic mechanical analysis studies conducted under electric field", IEEE Trans. Dielectr. Electr. Insul., Vol. 21, No. 5, pp. 2070–2080, 2014.

[14] R. R. Mocellini, O. A. Lambri, C. L. Matteo, J. A. García, G. I. Zelada-Lambri, P. A. Sorichetti, F. Plazaola, A. Rodríguez-Garraza and F. A. Sánchez, "Elastic misfit in two-phase polymer", Polymer, Vol. 50, No. 19, pp. 4696–4705, 2009.

[15] O. A. Lambri, F. Plazaola, E. Axpe, R. R. Mocellini, G. I. Zelada-Lambri, J. A. García, C. L. Matteo and P. A. Sorichetti, "Modification of the mesoscopic structure in neutron irradiated EPDM viewed through positron annihilation spectroscopy and dynamic mechanical analysis", Nucl. Inst. Meth. B., Vol. 269, No. 3, pp. 336–344, 2011.

[16] A.S.T.M. D3900-05a, "Rubber-Determination of Ethylene Units in Ethylene-Propylene Copolymers (EPM) and in Ethylene-Propylene-Diene Terpolymers (EPDM) by Infrared Spectrometry", ASTM Int. West Conshohocken, PA, USA, 2005.

[17] M. Celina, K. T. Gillen, J. Wise and R. L. Clough, "Anomalous aging phenomena in a crosslinked polyolefin cable insulation", Radiat. Phys. Chem., Vol. 48, No. 5, pp. 613–626, 1996.

[18] S. P. Yarmonenko, *Radiobiology*, MIR Publishers, Moscow, 1988.

[19] R. L. Sproull and W. A. Phillips, *Modern Physics: The Quantum Physics of Atoms, Solids and Nuclei*, John Wiley & Sons, New York, 1980.

[20] J. Kansy, "Microcomputer program for analysis of positron annihilation lifetime spectra", Nucl. Inst. Meth. A., Vol. 374, No. 2, pp. 235–244, 1996.

[21] M. Eldrup, D. Lightbody and J. N. Sherwood, "The temperature dependence of positron lifetimes in solid pivalic acid", Chem. Phys., Vol. 63, No. 1–2, pp. 51–58, 1981.

[22] H. Nakanishi, S. J. Wang and Y. C. Jean, *Positron Annihilation Studies of Fluids*, World Scientific, Singapore, 1988.

[23] Y. Y. Wang, H. Nakanishi, Y. C. Jean and T. C. Sandreczki, "Positron annihilation in amine-cured epoxy polymers—pressure dependence", J. Polym. Sci. Part B Polym. Phys., Vol. 28, No. 9, pp. 1431–1441, 1990.

[24] J. Liu, Q. Deng and Y. C. Jean, "Free-volume distributions of polystyrene probed by positron annihilation: comparison with free-volume theories", Macromolecules, Vol. 26, No. 26, pp. 7149–7155, 1993.
[25] Y. C. Jean, "Free-volume mean sizes of polymers probed by positron annihilation spectroscopy: a correlation of results obtained by PAL and by ACAR methods", Nucl. Inst. Meth. B., Vol. 56–57, pp. 615–617, 1991.
[26] H.-L. Li, Y. Ujihira, A. Nanasawa and Y. C. Jean, "Estimation of free volume in polystyrene-polyphenylene ether blend probed by the positron annihilation lifetime technique", Polymer., Vol. 40, No. 2, pp. 349–355, 1999.
[27] R. R. Mocellini, O. A. Lambri, F. G. Bonifacich, D. Gargicevich, F. Tarditti, M. Anhalt, B. Weidenfeller and W. Riehemann, "Electro-rheological Description of Solids Dielectrics Exhibiting Electrostriction", IEEE Trans. Dielectr. Electr. Insul., Vol. 23, No. 5, pp. 2993-3006, 2016.
[28] C. Darribere, *Collected Applications Thermal Analysis Elastomers*, METTLER-TOLEDO Collect. Appl., Vol. 1, pp. 49–50, 2001.
[29] L. M. Salvatierra, O. A. Lambri, C. L. Matteo, P. A. Sorichetti, C. A. Celauro and R. E. Bolmaro, "Growing of crystalline zones in EPDM irradiated with a low neutron flux", Nucl. Inst. Meth. B., Vol. 225, No. 3, pp. 297–304, 2004.
[30] O. A. Lambri, L. M. Salvatierra, F. A. Sánchez, C. L. Matteo, P. A. Sorichetti and C. A. Celauro, "Crystal growth in EPDM by chemi-crystallisation as a function of the neutron irradiation dose and flux level", Nucl. Inst. Meth. B., Vol. 237, No. 3, pp. 550–562, 2005.
[31] A. Charlesby, *Atomic Radiation and Polymers*, Pergamon Press, Oxford, pp. 579, 1960.
[32] A. Charlesby and L. Callaghan, "Crystallinity changes in irradiated polyethylenes", J. Phys. Chem. Solids, Vol. 4, No. 4, pp. 306–314, 1958.
[33] I. M. Ward and J. Sweeney, *Mechanical Properties of Solid Polymers. Chichester*, John Wiley & Sons, Ltd, West Sussex, 2012.
[34] J. Mark, K. Ngai, W. Graessley, L. Mandelkern, E. Samulski, J. Koenig and G. Wignall, *Physical Properties of Polymers*. 3rd Edition. Cambridge University Press, Cambridge, 2004.
[35] J. Davenas, I. Stevenson, N. Celette, G. Vigier and L. David, "Influence of the molecular modifications on the properties of EPDM elastomers under irradiation", Nucl. Inst. Meth. B., Vol. 208, pp. 461–465, 2003.
[36] Y. Long, R. A. Shanks and Z. H. Stachurski, "Kinetics of polymer crystallisation", Prog. Polym. Sci., Vol. 20, No. 4, pp. 651–701, 1995.
[37] J. D. Ferry, *Viscoelastic Properties of Polymers*, 3rd ed., John Wiley & Sons, Inc., New York, 1980.
[38] T. Mura, *Micromechanics of Defects in Solids*, Martinus Nijhoff, New York, 1987.
[39] J. D. Eshelby, "The Determination of the Elastic Field of an Ellipsoidal Inclusion, and Related Problems", Proc. R. Soc. A Math. Phys. Eng. Sci., Vol. 241, No. 1226, pp. 376–396, 1957.
[40] M. F. Ashby and D. R. Jones, *Engineering Materials, an Introduction to their Properties and Applications*, Pergamon Press, New York, 1980.

Federico Guillermo Bonifacich was born in Rosario, Argentina in 1988. He got his degree as electrical engineer from Rosario National University (UNR) in 2012 and the Ph.D. degree from the UNR in 2016. Nowadays he has got a fellowship from the National Council of Research of Argentina (CONICET). He also has a Doctoral position at the Laboratory of Materials (LEIM-CONICET) at the Electrical Engineering School (EIE) of the Faculty of Science and Engineering (FCEIA) of the UNR. He is focused on the study of ferromagnetic shape memory alloys and their applications in superelastic devices, sensors and actuators.

Enrique David Victor Giordano was born in Rosario, Argentina in 1983. He obtained his chemistry degree from the Pontifical Catholic University of Argentina (UCA) in 2008, and the Ph.D. degree (Chemistry) from the National University of Rosario (UNR) in 2014. Nowadays, he has got a fellowship from National Council for Research and Technology of Argentina (CONICET). He also has a post-doctoral position at the Institute of Biotechnological and Chemistry Processes (IPROBYQ), Faculty of Biochemical and Pharmaceutical Sciences. Currently, he is a chemistry professor at Pontifical Catholic University of Argentina. He is focused on the study of the relation of mechanical and electrical properties of polymer materials used in Electrical Industry.

Osvaldo Agustín Lambri was born in Rosario, Argentina in 1963. He obtained the B.Sc. and M.Sc. (physics, 1989) degrees from the Rosario National University (UNR) and the Ph.D. degree in physics (1993, focussed on materials science) from the same University. Post-doctoral position at the Laboratory of Materials in the University of the Basque Country, Bilbao, Spain. Guest Scientists at the Institut für Werkstoffkunde und Werkstofftechnick, Clausthal University of Technology, Clausthal Zellerfeld, Germany and at the Faculty of Science and Technology of the University of the Basque Country, Basque Country, Spain. Dr. Lambri is a member of the National Council of Research Staff of Argentina (CONICET). Since 2002 he is head of the Laboratory of Materials (LEIM) at the Electrical Engineering School (EIE) of the Faculty of Science and Engineering (FCEIA) of the UNR –CONICET. Since 2013 he is also head of the Centre of Electrical Technology (CETIE), FCEIA, UNR and since 2016 he is a Full Professor of Electrical Materials at EIE, FCEIA, UNR. He also was leader of Research Projects at the Institute Laue Langevin - Grenoble, France. His current research areas include the mechanical properties and phase transitions of super-alloys and refractory metals and the mechanical and electrical properties of polymers**.**

Damián Gargicevich was born in Casilda, Argentina in 1989. He got his degree as electrical engineer from Rosario National University (UNR) in 2012. Nowadays he has got a fellowship from the National Council of Research of Argentina (CONICET). He also has a Doctoral position at the Laboratory of Materials (LEIM-CONICET) at the Electrical Engineering School (EIE) of the Faculty of Science and Engineering (FCEIA) of the UNR.

Ricardo Raúl Mocellini, was born in San Lorenzo, Argentina in 1956. He got his degree as Electrical Engineer from Rosario National University (UNR) in 2006 and a Ph.D. degree from the same University in 2014. He is focused on the study of dielectric properties of technological materials. Dr. Mocellini is also an Associate Professor at EIE, FCEIA, UNR. He is also working at the Projects and Electrical Maintenance Department of Pampa Energia SA Plant in Puerto General San Martín, since 1992.

José Ángel. García was born in Bilbao, Spain in 1955. He obtained the B. Sc. and M. Sc. (Physics, 1977) from the University of the Basque Country. His Ph. D. degree work was realized at the J. J. Thompson Physical Laboratory of the Reading University in Great Britain. He spent several Post-Doctoral stages at Reading University and at the Science Faculty and Engineering of National University of Rosario in Argentina. At this time, he is responsible of the Optical Emission Spectroscopy Laboratory of the Science Faculty in the Basque Country in Leioa.

Fernando Plazaola Muguruza was born in Legorreta (Gipuzkoa), Spain in 1958. Graduated in physics (1982) from the Complutense University of Madrid. He had a pre-doctoral position in the Laboratory of Physics of the Helsinki University of Technology (HUT), Finland between 1982-85. He obtained the Ph. D. degree in physics (1986, focussed on materials science) from the University of the Basque Country (UPV/EHU). He was a Guest Scientist at the Helsinki University of Technology (HUT) in 1997. Since 1998 he is Full Professor of Applied Physics at the University of the Basque Country. Since 1999 he is the head of the laboratory of Nuclear Techniques applied to Material Science at the Science and Technology Faculty of the UPV/EHU. He has been visiting Professor at HUT (2003). Nowadays, he is Rector of Research of the University of the Basque Country. His current research areas include magnetic materials, defect studies in compound semiconductors and polymers**.**

Fernando Ariel Sánchez was born in Santa Fe (Argentina) in 1973. He studied physics in Rosario National University and reached the grade of Licenciate degree (M.Sc.) in 2000. After that, he performed a specialization of one year in Technological Applications of Nuclear Energy at Balseiro Institute (Bariloche). Since 2001, he works in neutronic and radiation transport in National Atomic Energy Commission at Bariloche Atomic Center. His main experience is in research reactor technology, experimental applications, neutronic design.

Carlos Eugenio Boschetti was born in Rosario, Argentina in 1965. He obtained his chemistry degree from the National University of Rosario (UNR) in 1991, and the Ph.D. degree (Chemistry) from the same University in 1995. He had post-doctoral positions at the Dept. of Organic Chemistry in the University of the Basque Country, Donostia, and then at the Dept. of Chemistry in the University of Cambridge, UK, as a Marie Curie Fellow (European Commission). After spending some time in the R+D Department of a petrochemical company, he gained in 2004 a position as Researcher in the National Council for Research and Technology of Argentina (CONICET). He has had many teaching positions in the Faculty of Biochemical and Pharmaceutical Sciences in the National University of Rosario, being currently an Associate Professor in the Chemical Technology Area at the same Faculty. His current research areas include analytical and process chemistry on polymers and polymerization.

Pablo Ernesto Salvatori was born in Peyrano, Argentina in 1990. He received his degree in Chemistry from the National University of Rosario (UNR) in 2014, and he is currently doing the Ph.D. degree at the same University. He has also a fellowship from the National Research Council of Argentina (CONICET) in collaboration with Pampa Energia SA (Argentina). His research is focused on the development and properties of synthetic rubber compounds for specific applications.